Extended Data Figure 1

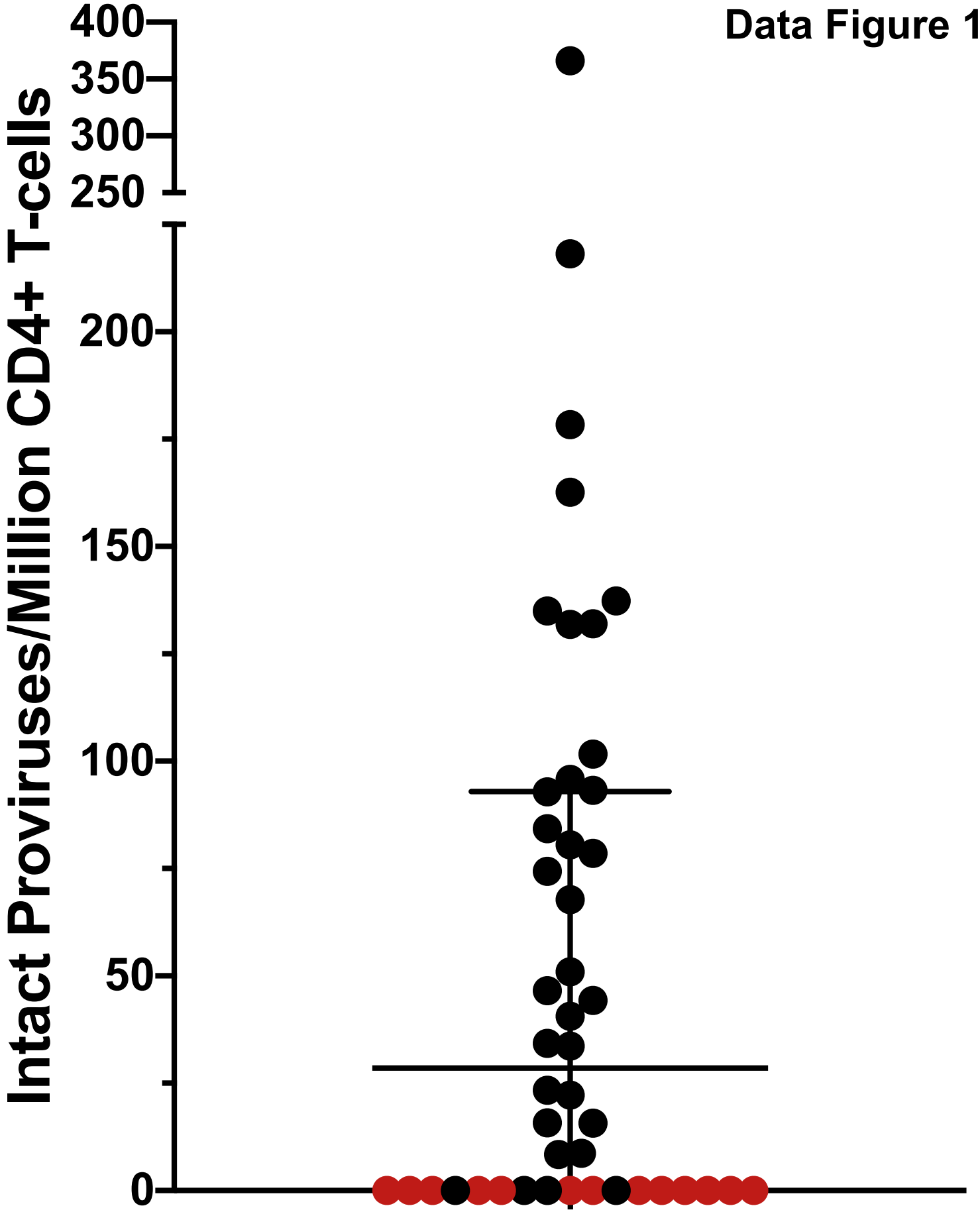

Extended Data Figure 1: IPDA results for 46 study participants. Line and error bars indicate cohort median and interquartile range; red datapoints represent 13 presumed instances of IPDA detection failure.

Extended Data Figure 2

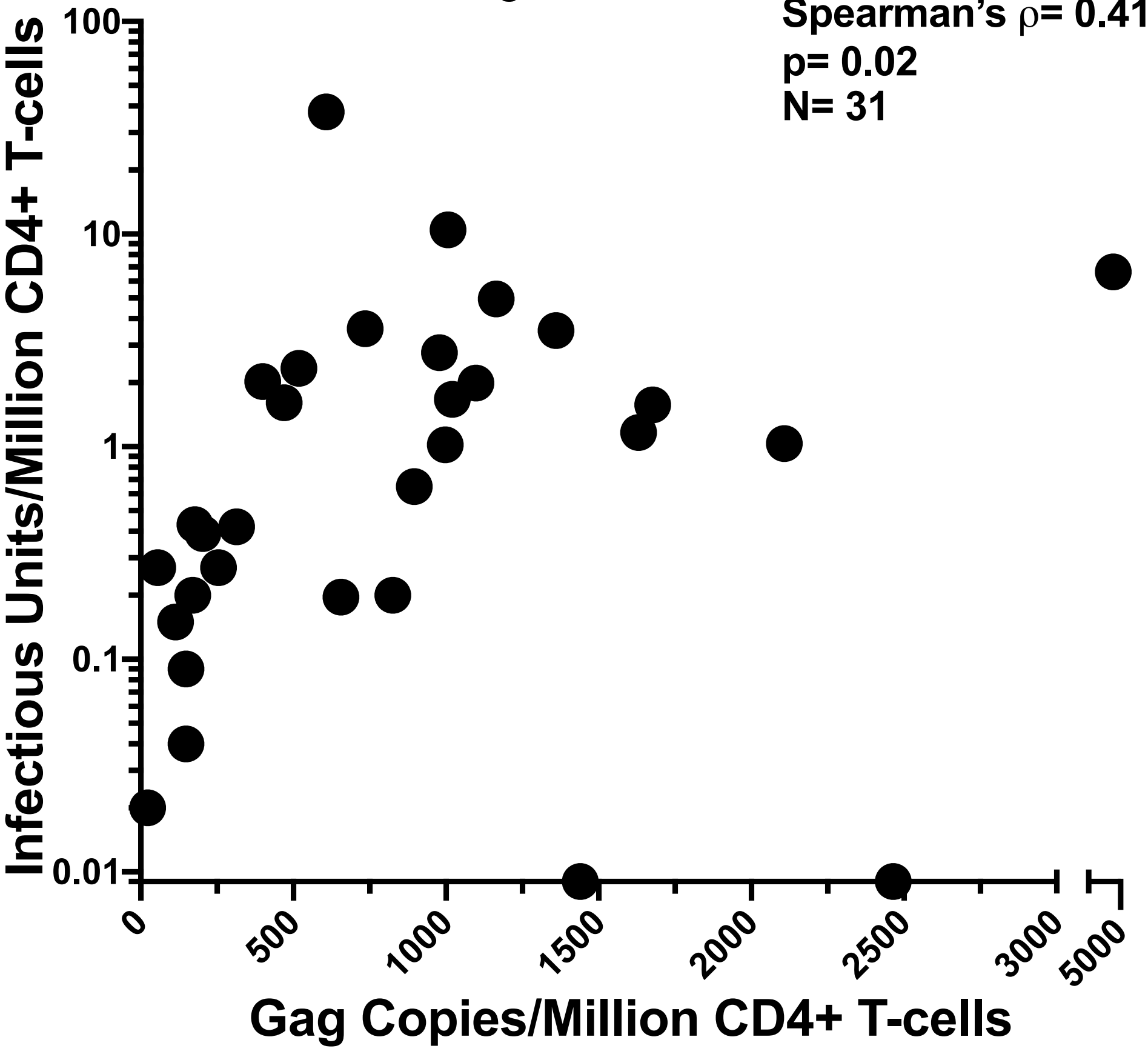

Extended Data Figure 2: Spearman's correlation between QVOA and HIV *gag* copies/million CD4+ T-cells in a North American cohort. Data were available for N=31 participants. Two individuals for whom no replication competent viruses were detected (IUPM= 0) are plotted on the X-axis.

Extended Data Figure 3

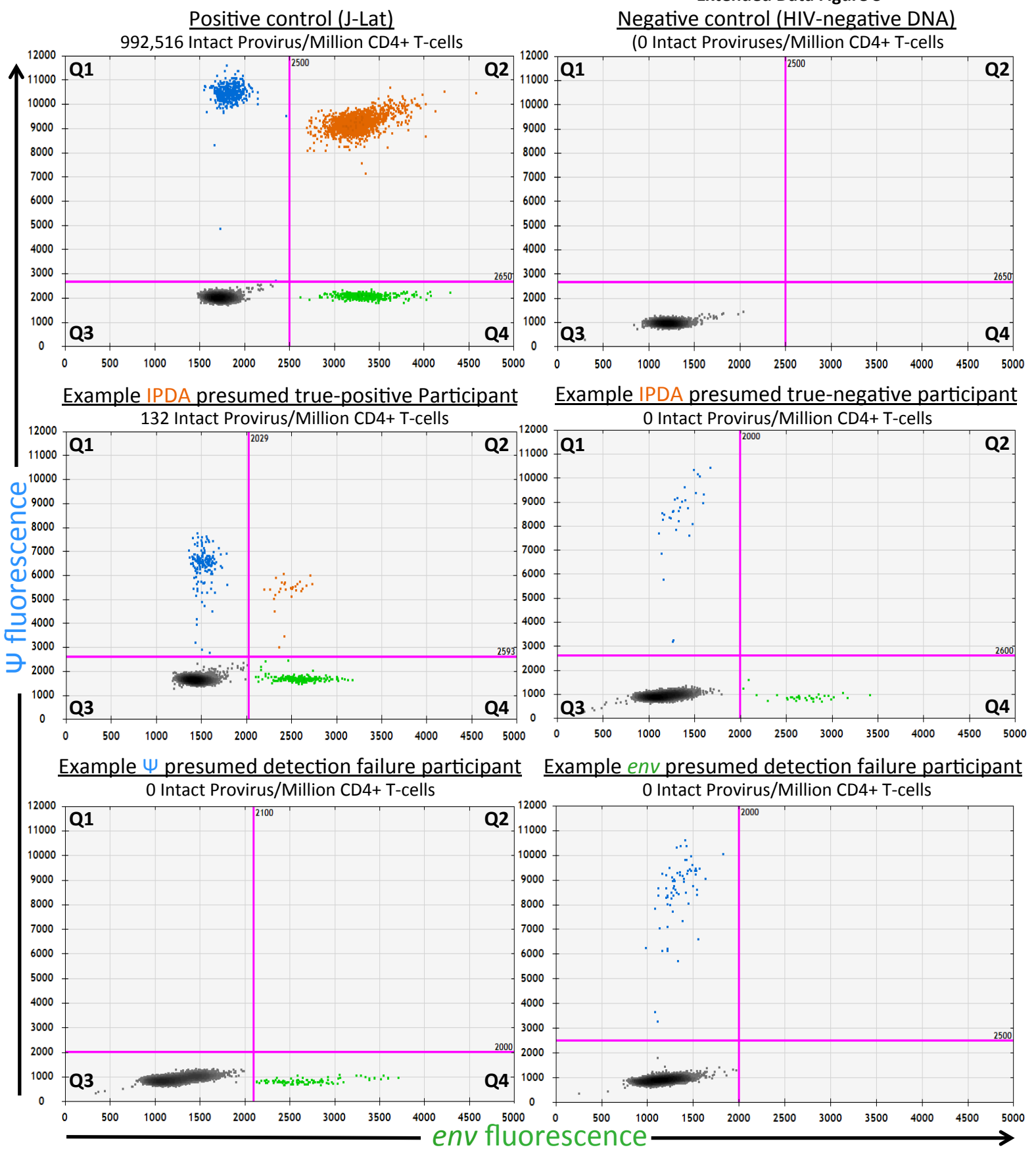

Extended Data Figure 3: Example IPDA 2D plots for control and participant samples. 2D ddPCR plots showing Ψ-single positive events (Q1, blue), Ψ- and *env*-double positive events (Q2, orange), double-negative events (Q3, grey) and *env*-single positive events (Q4, green), for positive control J-Lat cell line (top left; 1 copy of HIV per cell, droplets in Q1 and Q4 are a result of anticipated DNA shearing that occurs during DNA extraction that is subsequently corrected mathematically based on RPP30 shearing); HIV-negative donor negative control (top right); IPDA true-positive participant (middle left); IPDA true-negative participant (middle right) and IPDA detection failures (bottom row). Plots show merge of replicate wells.

Ext Data Figure 4

Ψ sequence polymorphisms in IPDA Ψ detection failure samples

ID	Ψ Forward Primer CAGGACTCGGCTTGCTGAAG	Ψ Probe ACTGGTGAGTACGCCAAAA	Ψ Reverse Primer GCTAGAAGGAGAGAGATGGGTGC
HGLK001	----------GC	----------T	----------
OM5365	----------GC	R----------TT	----------
WWH-012	----------GC	----------	----------
WWH-031	----------A---	-ACA--A----------TT	-------A------A--A-----
BC-014	----------	-AC----------	----------

env sequence polymorphisms in IPDA *env* detection failure samples

ID	*env* Forward Primer AGTGGTGCAGAGAGAAAAAAGAGC	*env* Probe CCTTGGGTTCTTGGGA	*env* Reverse Primer GCTGACGGTACAGGCCAGAC
HGLK002	----------G------	---C--------ATC-	----------R-
HGLK005	----------*R-K---G------	---C----------	----------R-------
CIENI223	----------	-----C----------	----------R-------
OM5334	----------G--------	------A---------	----------R------
CIRC0333	----------	---------T------	----------A
WWH-011	----------G	----------	----------
WWH-026	----------	------T---------	----------
WWH-031	----------	---G-----TC-----	----------
BC-004	---------A----------	---------YC-----	----------

* = ATGCWR insertion prior to R

Extended Data Figure 4: HIV polymorphism in IPDA primer/probe binding sites.

Primer and probe region sequences for participants with Ψ (top) or *env* (bottom) detection failure. Hyphens **(–)** indicate matches to the IPDA primer or probe; red letters indicate mismatches; asterisk indicates the location of an insertion.

Extended Data Figure 5

91C33

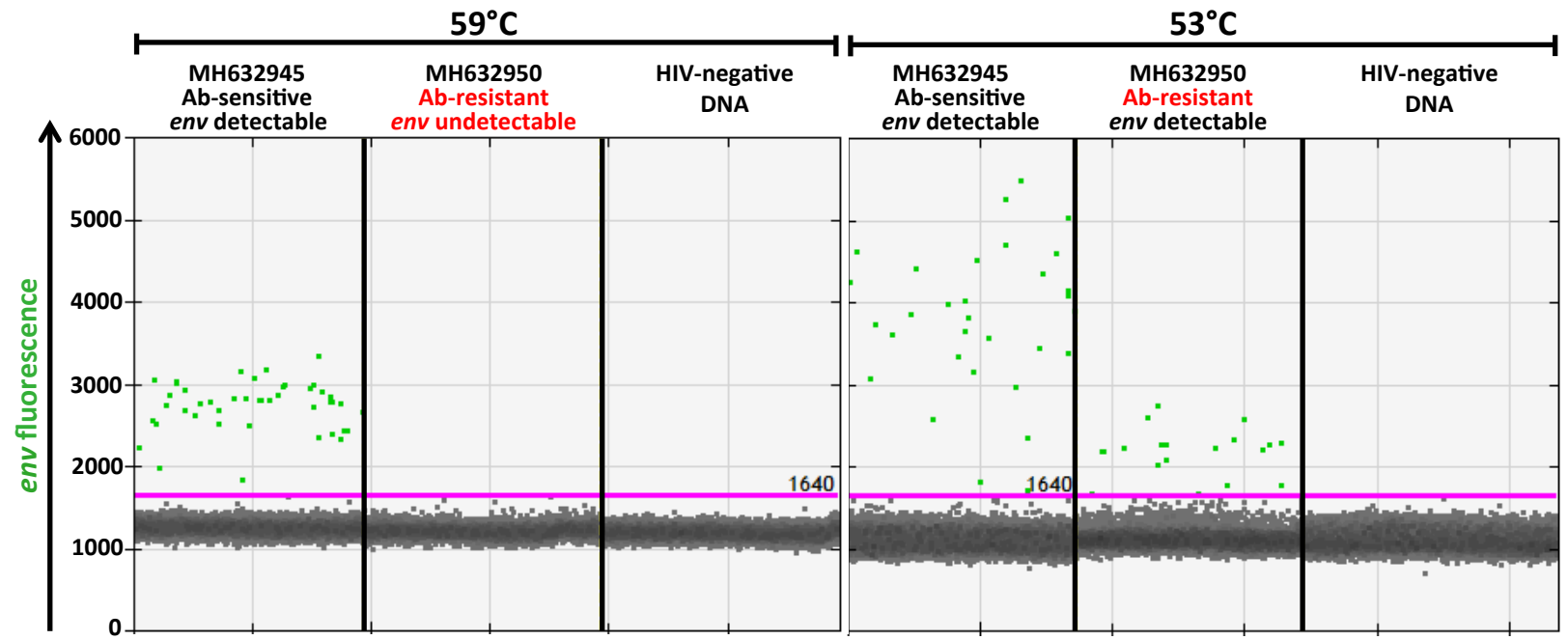

Input DNA :	$7.5x10^{-8}$ ng	$1x10^{-7}$ ng	0.19 ng	$7.5x10^{-8}$ ng	$1x10^{-7}$ ng	0.19 ng
IPDA-measured concentration : (copies/µl rxn)	2.7	0	0	2.3	1.3	0

Extended Data Figure 5: Modification of published IPDA conditions to reduce assay stringency allows for detection of 91C33 mismatch variant. Representative ddPCR IPDA *env* plots for MH632945 (representing 91C33's bNAb-sensitive, IPDA *env* probe-matching HIV population) and MH632950 (representing 91C33's bNAb-resistant, IPDA env probe-mismatched HIV population); positive droplets are green and negative droplets are grey. Templates were purified *env* PCR products of equal length and comparable quantities. HIV-negative donor DNA served as a negative control. (left): results under published conditions; (right): result when assay annealing/extension temperature was reduced to 53°C.

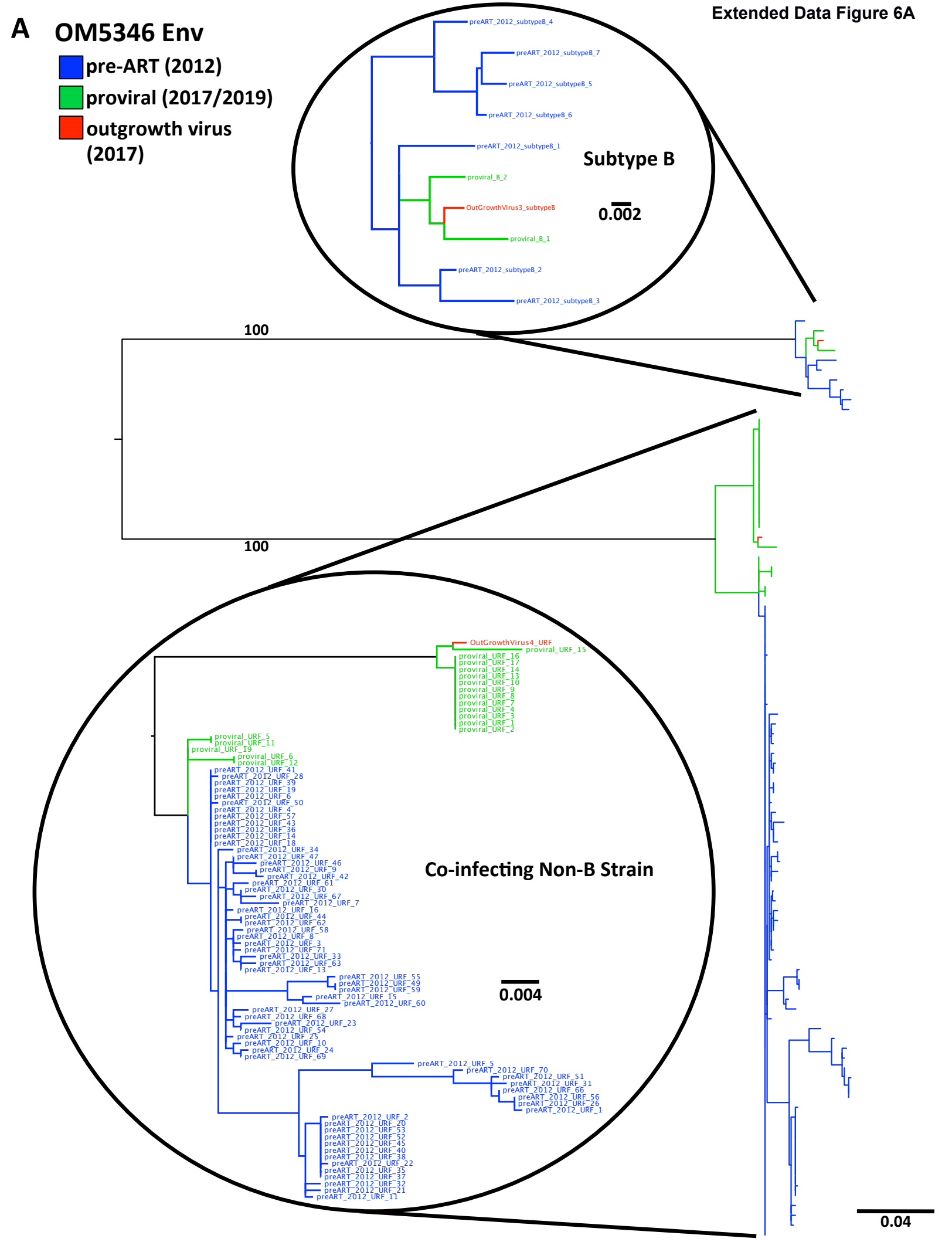
A
OM5346 Env
pre-ART (2012)
proviral (2017/2019)
outgrowth virus (2017)
preART_2012_subtypeB_4
preART_2012_subtypeB_7
preART_2012_subtypeB_5
preART_2012_subtypeB_6
preART_2012_subtypeB_1
proviral_B_2
OutGrowthVirus3_subtypeB
proviral_B_1
preART_2012_subtypeB_2
preART_2012_subtypeB_3
Subtype B
0.002
100
100
OutGrowthVirus4_URF
proviral_URF_15
proviral_URF_16
proviral_URF_17
proviral_URF_14
proviral_URF_13
proviral_URF_10
proviral_URF_9
proviral_URF_8
proviral_URF_7
proviral_URF_4
proviral_URF_3
proviral_URF_1
proviral_URF_2
proviral_URF_5
proviral_URF_11
proviral_URF_19
proviral_URF_6
proviral_URF_12
preART_2012_URF_41
preART_2012_URF_28
preART_2012_URF_39
preART_2012_URF_19
preART_2012_URF_6
preART_2012_URF_50
preART_2012_URF_4
preART_2012_URF_57
preART_2012_URF_43
preART_2012_URF_36
preART_2012_URF_14
preART_2012_URF_18
preART_2012_URF_34
preART_2012_URF_47
preART_2012_URF_46
preART_2012_URF_9
preART_2012_URF_42
preART_2012_URF_61
preART_2012_URF_30
preART_2012_URF_67
preART_2012_URF_7
preART_2012_URF_16
preART_2012_URF_44
preART_2012_URF_62
preART_2012_URF_58
preART_2012_URF_8
preART_2012_URF_3
preART_2012_URF_71
preART_2012_URF_33
preART_2012_URF_63
preART_2012_URF_13
preART_2012_URF_55
preART_2012_URF_49
preART_2012_URF_59
preART_2012_URF_15
preART_2012_URF_60
preART_2012_URF_27
preART_2012_URF_68
preART_2012_URF_23
preART_2012_URF_54
preART_2012_URF_25
preART_2012_URF_10
preART_2012_URF_24
preART_2012_URF_69
preART_2012_URF_5
preART_2012_URF_70
preART_2012_URF_51
preART_2012_URF_31
preART_2012_URF_66
preART_2012_URF_56
preART_2012_URF_26
preART_2012_URF_1
preART_2012_URF_2
preART_2012_URF_20
preART_2012_URF_53
preART_2012_URF_52
preART_2012_URF_45
preART_2012_URF_40
preART_2012_URF_38
preART_2012_URF_22
preART_2012_URF_35
preART_2012_URF_37
preART_2012_URF_32
preART_2012_URF_21
preART_2012_URF_11
Co-infecting Non-B Strain
0.004
0.04

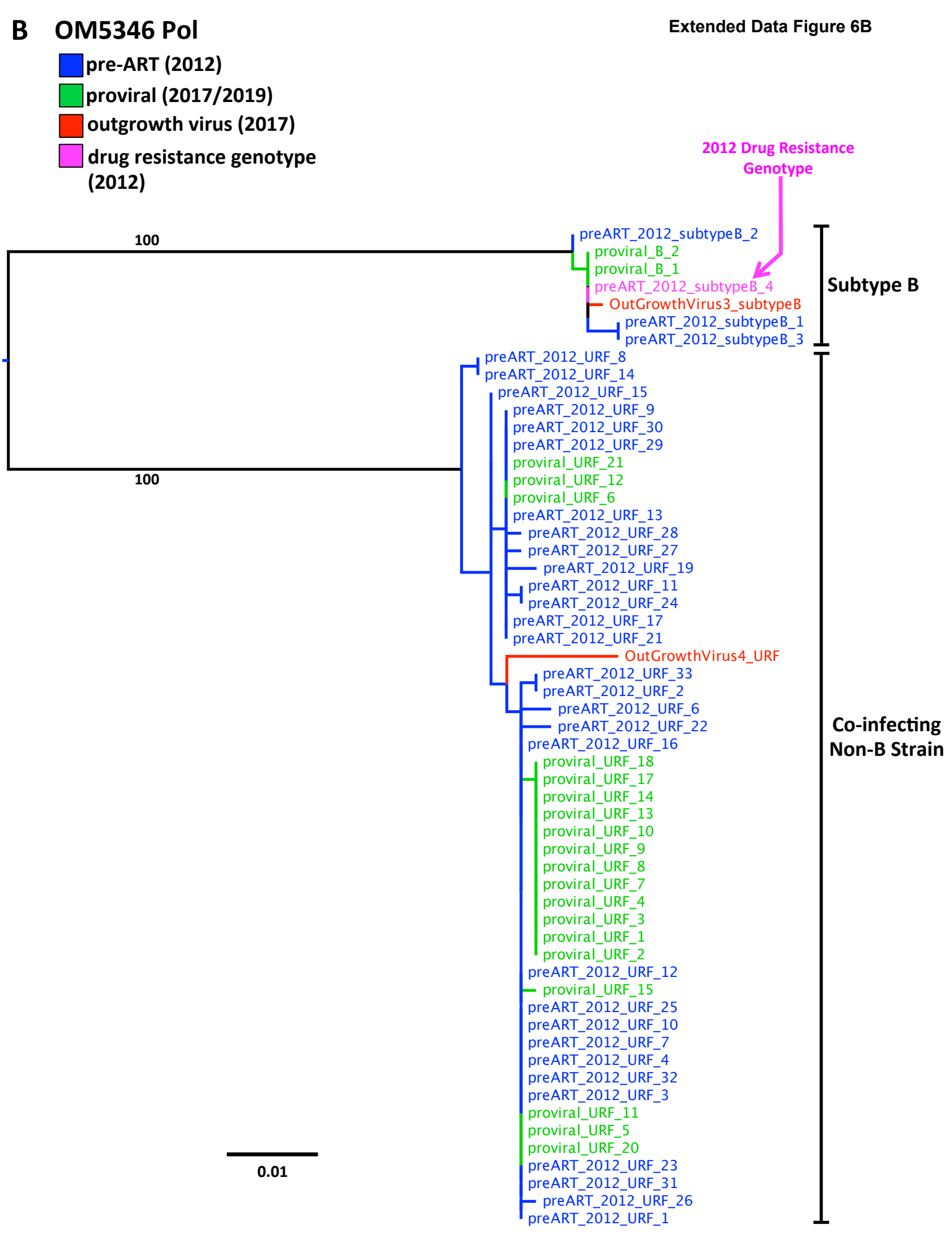
B OM5346 Pol
pre-ART (2012)
proviral (2017/2019)
outgrowth virus (2017)
drug resistance genotype (2012)
2012 Drug Resistance Genotype
100
100
preART_2012_subtypeB_2
proviral_B_2
proviral_B_1
preART_2012_subtypeB_4
OutGrowthVirus3_subtypeB
preART_2012_subtypeB_1
preART_2012_subtypeB_3
Subtype B
preART_2012_URF_8
preART_2012_URF_14
preART_2012_URF_15
preART_2012_URF_9
preART_2012_URF_30
preART_2012_URF_29
proviral_URF_21
proviral_URF_12
proviral_URF_6
preART_2012_URF_13
preART_2012_URF_28
preART_2012_URF_27
preART_2012_URF_19
preART_2012_URF_11
preART_2012_URF_24
preART_2012_URF_17
preART_2012_URF_21
OutGrowthVirus4_URF
preART_2012_URF_33
preART_2012_URF_2
preART_2012_URF_6
preART_2012_URF_22
preART_2012_URF_16
proviral_URF_18
proviral_URF_17
proviral_URF_14
proviral_URF_13
proviral_URF_10
proviral_URF_9
proviral_URF_8
proviral_URF_7
proviral_URF_4
proviral_URF_3
proviral_URF_1
proviral_URF_2
preART_2012_URF_12
proviral_URF_15
preART_2012_URF_25
preART_2012_URF_10
preART_2012_URF_7
preART_2012_URF_4
preART_2012_URF_32
preART_2012_URF_3
proviral_URF_11
proviral_URF_5
proviral_URF_20
preART_2012_URF_23
preART_2012_URF_31
preART_2012_URF_26
preART_2012_URF_1
Co-infecting Non-B Strain
0.01

Extended Data Figure 6: *Env* and *pol* phylogenies for participant OM5346, who is co-infected with two HIV strains. (A). Maximum likelihood phylogeny inferred from single-genome-amplified *env* RNA sequences from pre-ART plasma (2012, blue), proviruses sampled on ART (2017 and 2019, green) and replication competent HIV sequences isolated from the reservoir (2017, red). **(B).** The *pol* phylogeny additionally includes a sequence from a clinical HIV drug resistance test performed in 2012 (pink). *Pol* sequences of replication-competent reservoir sequences (2017, red) were recovered from cells infected with these viruses *in vitro*. Scale bars indicate substitutions per nucleotide site. Numbers on main branches indicate branch support values.

Extended Data Figure 7

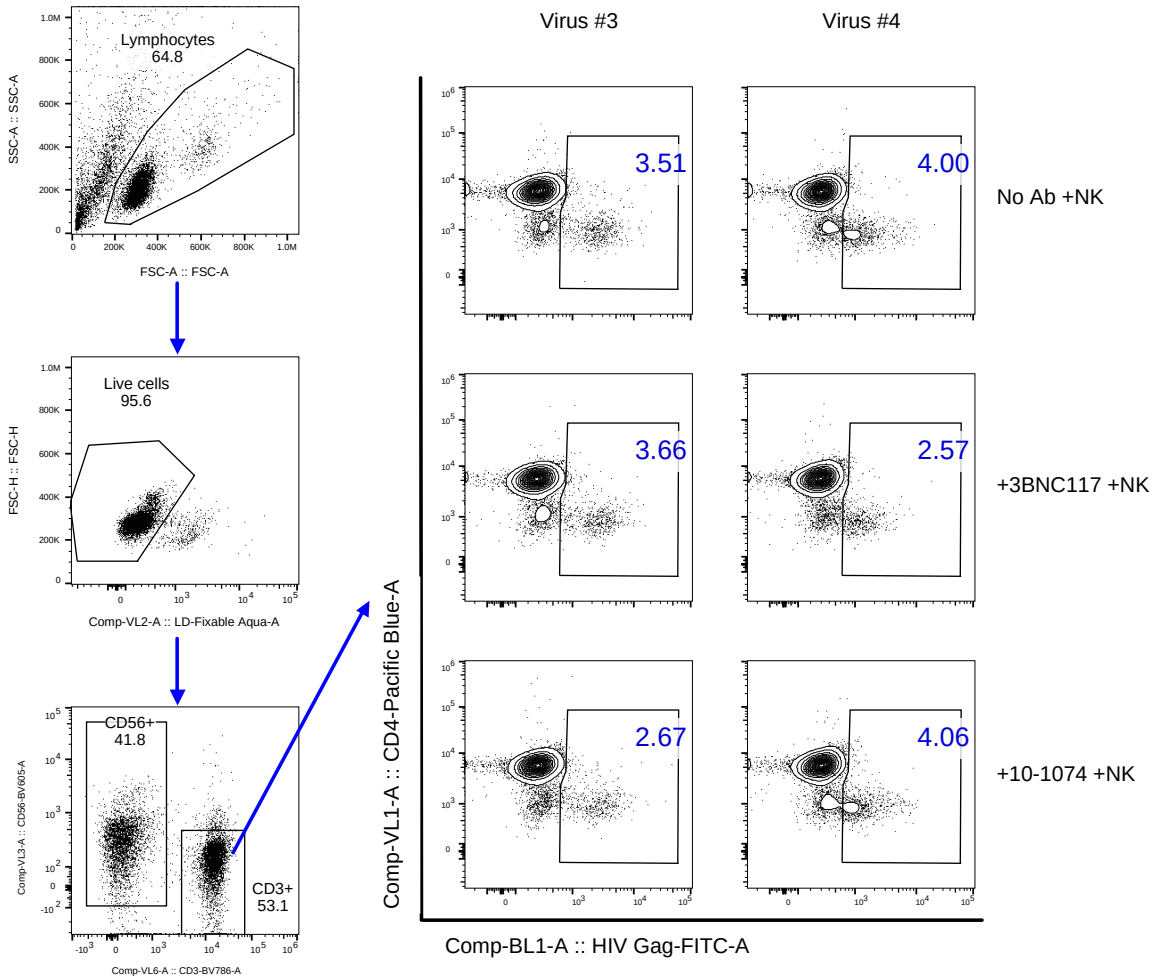

Extended Data Figure 7: OM5346 ADCC gating strategy. Representative flow plots showing flow cytometry gating strategy: Lymphocytes -> live cells (live/dead dye-) -> NK cells ($CD56^+$) and T-cells ($CD3^+$) -> HIV-positive cells (HIV Gag^+) from T-cell population. Activated $CD4^+$ T-cells from an HIV-negative donor were infected with OM5346 virus 3 (left) or virus 4 (right). NK cells were isolated from an HIV-negative donor. Plots on the top row show $CD4^+$ T-cells in control experiments (with no bNAb or NK cells added), 2nd row shows $CD4^+$ T cells remaining after addition of NK cells only, 3rd row shows $CD4^+$ T cells remaining after addition of 3BNC117 and NK cells, 4th row shows $CD4^+$ T cells remaining after addition of 10-1074 and NK cells. CD4 downregulation in HIV-positive cells (HIV Gag^+) occurs due to Nef-induced CD4 downregulation.

A Ext Data Figure 8

Virus-infected cells: No detection of OM5346 Virus 4 by IPDA

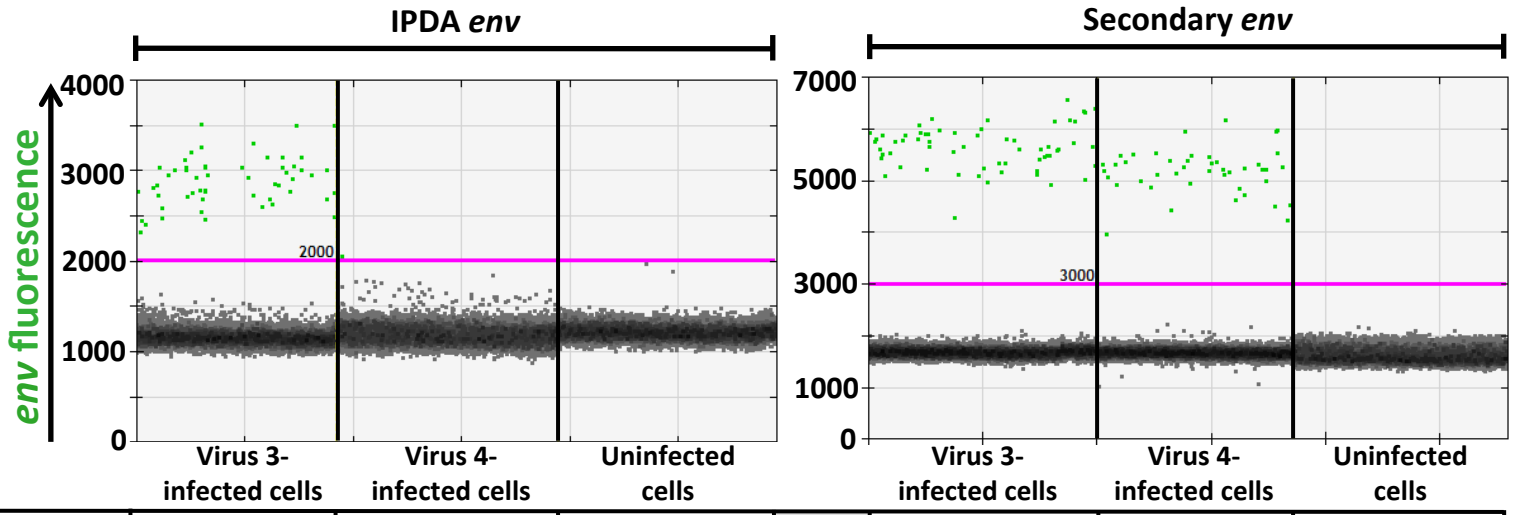

input DNA	0.75 ng	0.75 ng	0.75 ng		0.75 ng	0.75 ng	0.75 ng
IPDA-measured concentration (copies/µl rxn)	3.6	0.06	0		3.6	3.1	0

B

Detection of Virus 4 pure template at high, but not participant-*like*, concentrations

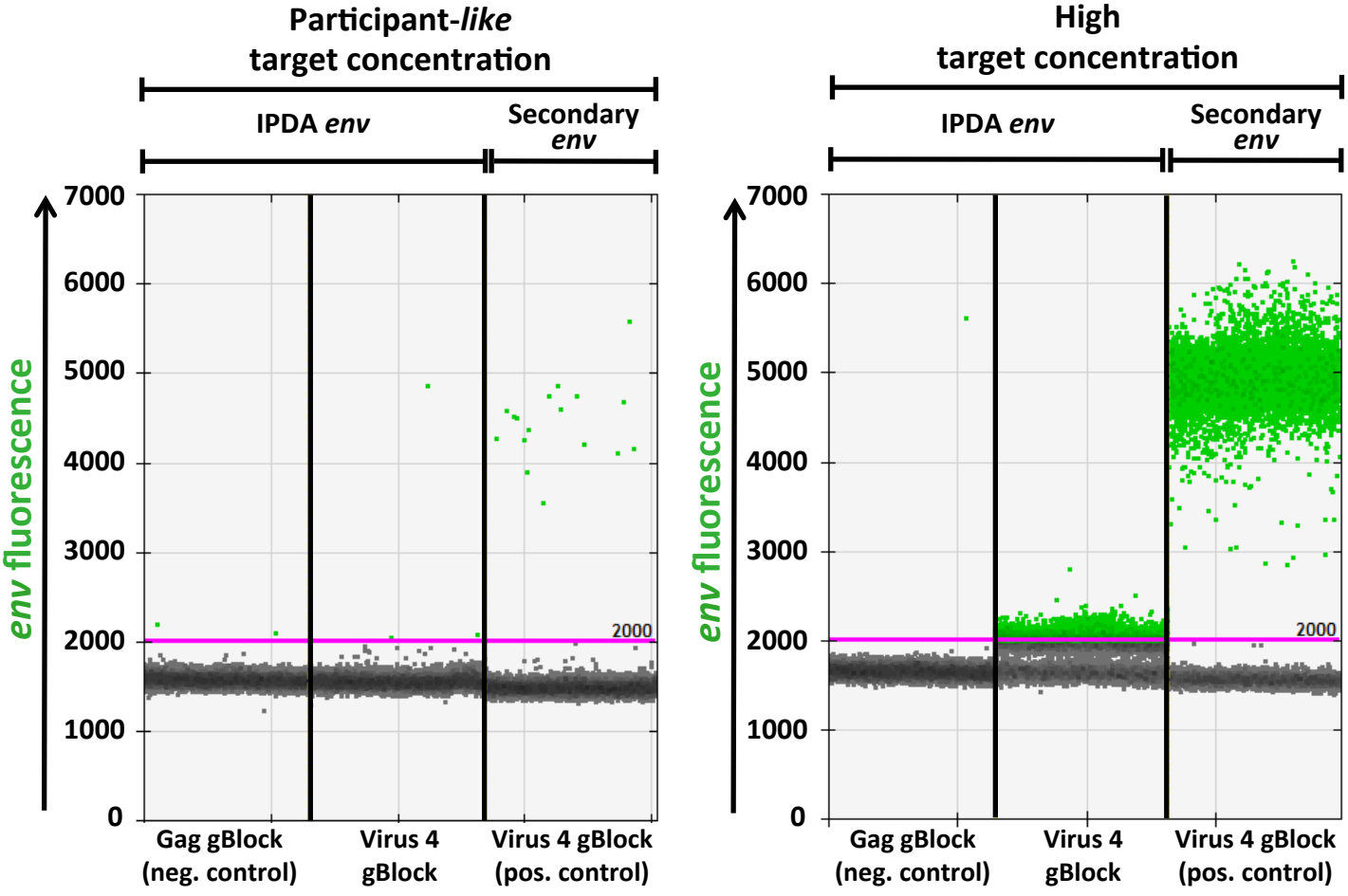

input DNA (nmol)	$1x10^{-6}$	$1x10^{-6}$	$1x10^{-6}$		$6.7x10^{-4}$	$6.7x10^{-4}$	$6.7x10^{-4}$
IPDA-measured concentration (copies/µl rxn)	0.18	0.25	1.5		0.09	456	914

Extended Data Figure 8: OM5346 Virus 4 sequence is undetectable by the IPDA at participant-like concentrations. (A). Representative 1D *env* plots using IPDA (left) or the secondary *env* reaction (right), from $CD4^+$ T-cells infected with OM5346 virus 3 (IPDA *env* probe match), virus 4 (IPDA *env* probe G13A mismatch) or uninfected cells (negative control). Positive droplets are green; negative droplets are grey. Copies/μl reaction as calculated from the experimental data are shown below the plots. The left panel is the same as Figure 2B. **(B).** Representative 1D *env* plots of OM5346 virus 4, tested as a synthetic DNA gene fragment ("Virus 4 gBlock"), using IPDA and secondary *env* reactions, at different input concentrations. A Gag synthetic gene fragment ("Gag gBlock") served as the negative control. Input DNA quantity and copies/μl reaction as calculated from the experimental data are shown below the plot. These observations provide a possible explanation to reconcile the original authors' ability to detect this sequence using a pure plasmid template and our inability to detect it at conditions mimicking a participant sample.

Extended Data Figure 9

A

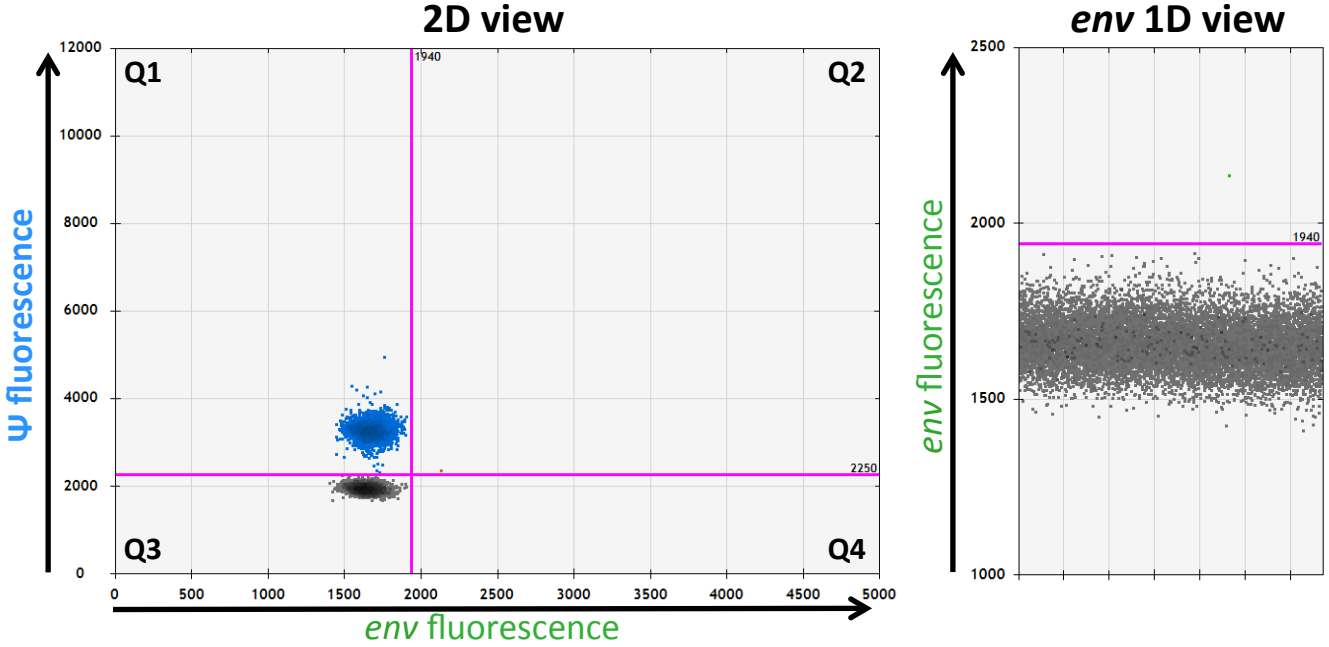

B

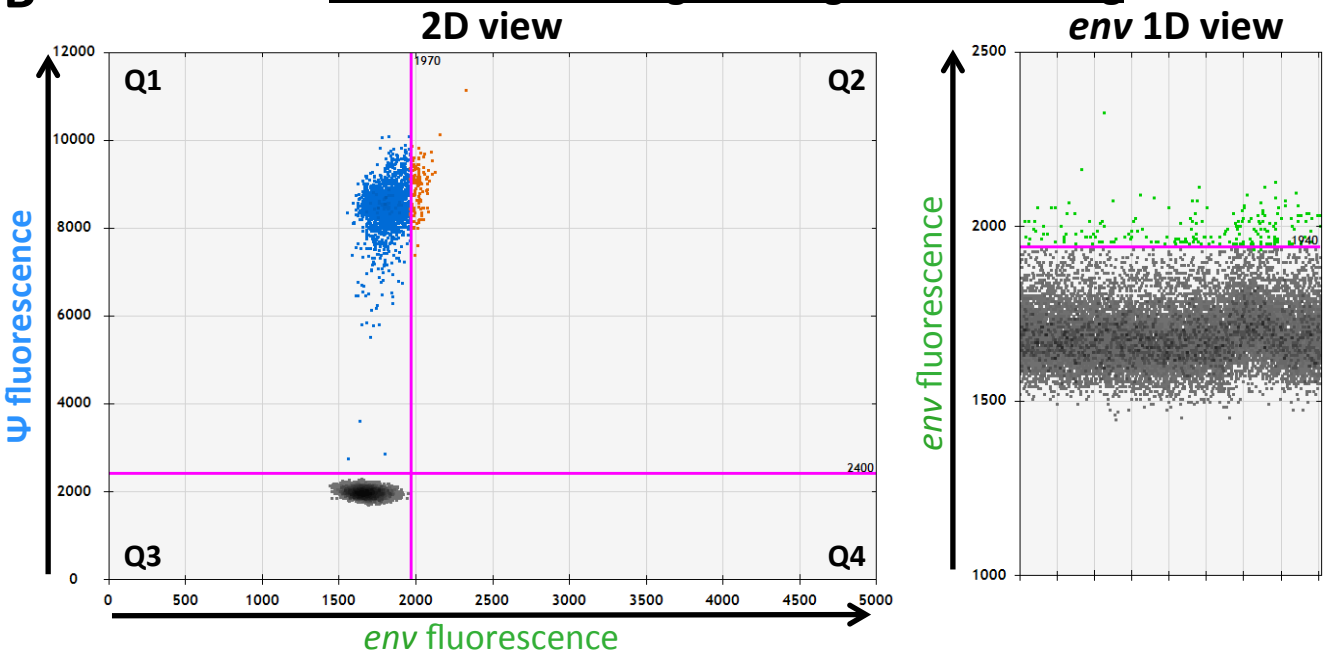

C

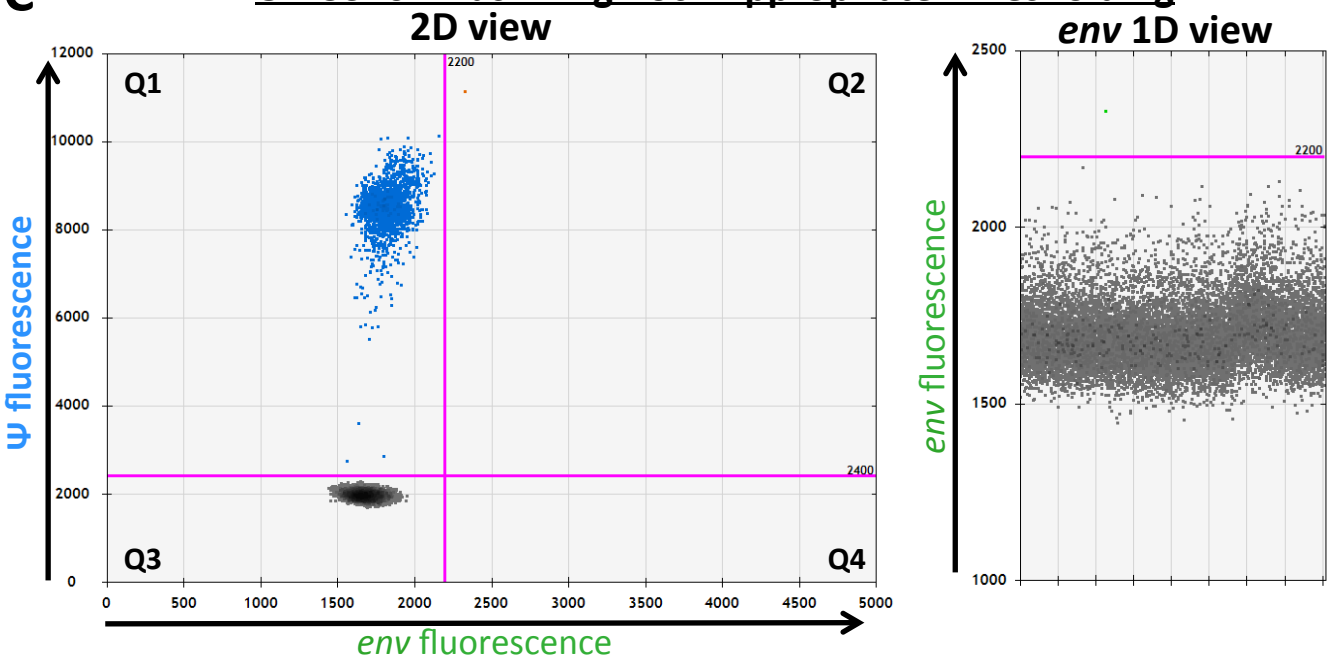

Extended Data Figure 9: Sequence-specific fluorescence spillover prohibits tight thresholding on negative populations in the IPDA. (A) 2D (left) and *env* 1D (right) plots of OM5346 virus 3 Ψ region sequence, tested as a synthetic DNA gene fragment ("Virus 3 Ψ gBlock") without corresponding *env* template. Minimal Ψ- to *env*- channel spillover occurs when drawing the positive droplet threshold tightly to the double negative population (note the presence of one false-double positive droplet). **(B)** 2D (left) and *env* 1D (right) plots of OM5346 virus 4 Ψ region sequence, tested as a synthetic DNA gene fragment ("Virus 4 Ψ gBlock"), without corresponding *env* template. With this sequence, drawing of a tight threshold yields marked spillover of Ψ (FAM) fluorescence into the *env* (VIC) channel, yielding false-positive *env* (and by extension, false-positive intact) signal. **(C)** 2D (left) and *env* 1D (right) plots of OM5346 Virus 4 Ψ region sequence, tested as a synthetic DNA gene fragment ("Virus 4 Ψ gBlock") without corresponding *env* template, with a threshold drawn at an appropriate distance from the double negative population. This threshold accommodates the sequence-specific shift in the Ψ-positive to avoid the creation of false-positive intact or *env*-positive droplet population (note the presence of a single false-double positive droplet).

Ext Data Figure 10

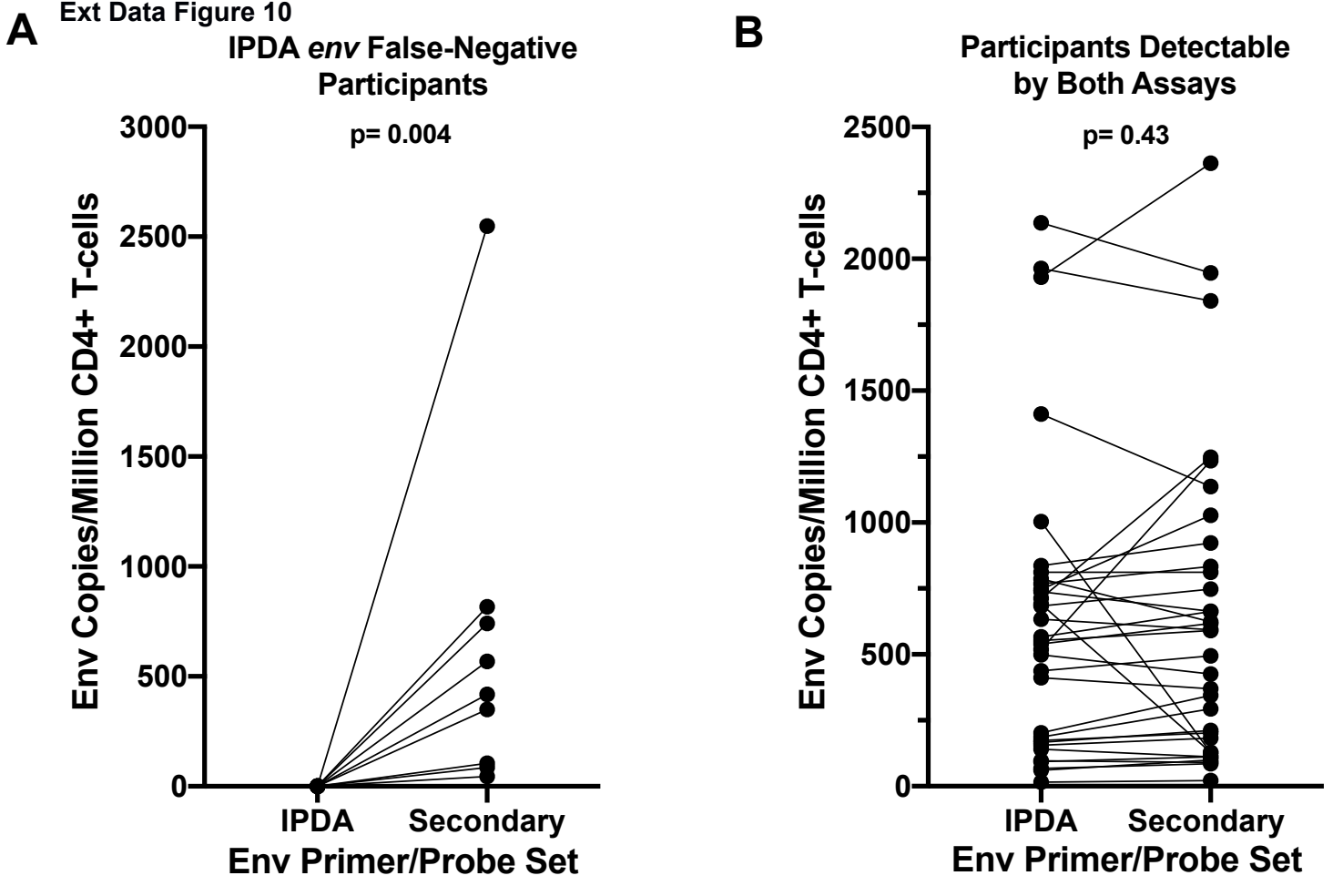

Extended Data Figure 10: Performance of the secondary *env* primer/probe set. (A) A secondary *env* primer/probe set rescued detection in all 9 cases of IPDA *env* detection failure **(B)** In 33 participants whose reservoir was detectable by both IPDA and secondary *env* primer/probe sets, measurements showed no significant differences by Wilcoxon signed-rank test.

Ext Data Figure 11

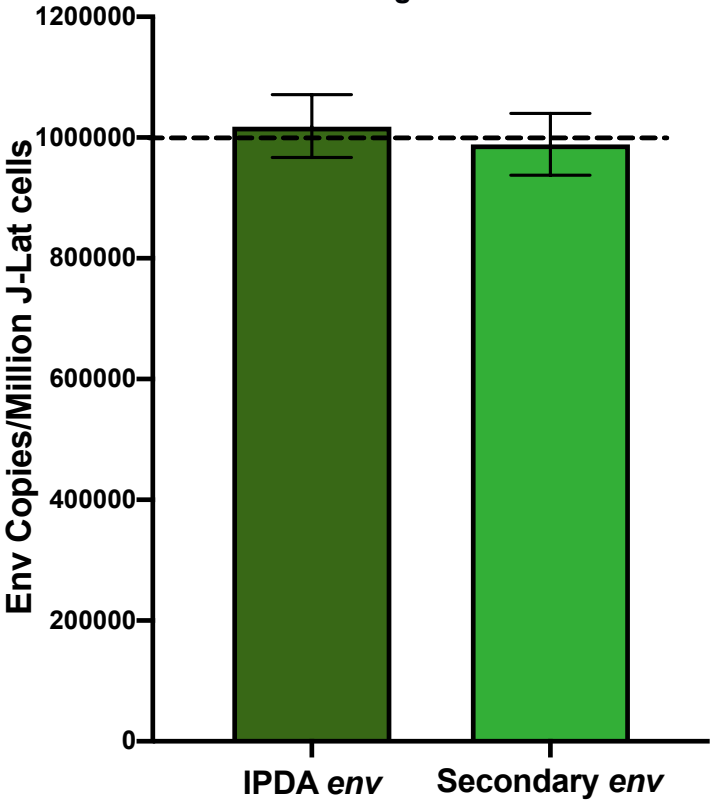

Extended Data Figure 11: Comparable detection of expected 1:1 HIV-to-Cell ratio in J-Lat cells by IPDA and Secondary *env* reactions. Error bars indicate 95% total Poisson confidence interval.